

## Semiclassical image potential at a solid surface

P. M. Echenique\*

*Oak Ridge National Laboratory, Oak Ridge, Tennessee 37830*

R. H. Ritchie

*Oak Ridge National Laboratory, Oak Ridge, Tennessee 37830  
and Department of Physics, University of Tennessee, Knoxville, Tennessee 37916*

N. Barberán

*Facultad de Física, Universidad de Barcelona, Barcelona, Spain*

John Inkson

*Cavendish Laboratory, Cambridge CB3 0HE, England*

(Received 10 October 1979)

A surface dielectric function of a semi-infinite plane-bounded metal is defined in the spirit of the plasmon-pole dielectric function of the bulk. It is modeled in such a way that the surface-plasmon dispersion relation is recovered for small momentum transfer. This function is employed to compute the image potential at all distances outside the surface. Interaction with bulk modes is neglected for simplicity and clarity. The interaction of a massive point charge with a metal surface is also considered in the context of a boson model for surface-plasmon excitation. We present a new definition of the image potential for this case.

### INTRODUCTION

A charged particle approaching a solid surface experiences a potential arising from the polarization it induces in the medium. This complex potential corresponds to the self-energy of the incident particle due to its interaction with surface modes, and the real part of this potential is due to virtual excitation of such modes. Real processes (i.e., creation of surface excitations via inelastic scattering) are responsible for the imaginary part of the potential.

When the particle is far away from the surface, it couples to long-wavelength collective modes of the system. The importance of surface modes to the image potential was emphasized independently by Lucas,<sup>1</sup> Mahan,<sup>2</sup> Ritchie,<sup>3</sup> and Feibelman.<sup>4</sup> This followed the earlier discovery that van der Waals forces also have their origin in surface modes.<sup>5,6</sup> Dynamical corrections to the image potential have been subject of considerable interest.<sup>7-9</sup> All these investigations have focused on the real part of the surface potential without including dispersion of the surface modes. The effect of dispersion upon the real part of the potential has been studied by Harris and Jones,<sup>10</sup> Heinrichs,<sup>11</sup> and more recently by Chan and Richmond.<sup>12</sup> They find that for small distances from the surface, dispersion effects can alter significantly the image potential with respect to the undispersed case.

Recent developments in the field of low-energy

electron diffraction<sup>13,14</sup> have shown the importance of obtaining a good one-electron complex optical potential at distances close to the surface where single-particle excitations become important. Quantum-mechanical treatments have been proposed<sup>15-18</sup> but result in a formalism much less transparent than the classical theory. The results are quite complicated and are probably too cumbersome for use in low-energy electron diffraction (LEED) and reflection high-energy electron diffraction (RHEED) calculations. Flores and Garcia-Moliner<sup>19</sup> have derived recently a formula for the complex self-energy, valid for an arbitrary dielectric function both within a semiclassical and a quantum formulation. We present in this paper a model for the surface dielectric function that includes collective effects and single-particle effects, being at the same time simple enough so that the potentials derived from it may be used readily in a number of surface-related problems.

In all of the work presented here, we neglect interactions with bulk modes for emphasis and for simplicity. Their effect is negligible until the particle is very close ( $z \lesssim 1$  a.u.) to the solid. These interactions could be included in a straightforward way and in our linear approximation give a simple additive effect that is important only inside the solid, tending to cancel the surface-plasmon contributions there. This neglect implies that our results are valid only when the charged particle is outside of the solid. In addition, Eq. (1) below applies only when this is true, since

use of the specular reflection boundary condition results in a different formula when  $z > 0$ . We display the surface contribution to the image potential in several graphs below. The contribution from these modes is asymmetric with respect to the surface when the charge is in motion because of the possibility of real excitation. The graphs of the image potential  $\Phi_I$  (and  $\Sigma_{i1}$  in Fig. 4) are to be interpreted as follows. Values for  $z < 0$  correspond to the image potential for a charged particle approaching the surface. Values for  $z > 0$  correspond to the image potential for a charged particle emerging from the metal into vacuum.

First we introduce an approximation to the surface dielectric constant and illustrate its use by calculating the static image potential. Next we recast the problem in a Hamiltonian formalism which allows us to separate effects associated with virtual and real processes (i.e., with the real and imaginary part of the surface potential). There seems to be some ambiguity about this point in the literature.<sup>7,20</sup>

$$\Phi_I(z) = -\frac{Z_1^2 v_{\perp}}{4\pi^2} \int d^2Q \int_{-\infty}^{\infty} d\omega e^{i(\vec{Q}\cdot\vec{v}-\omega)z/v_{\perp}} \frac{e^{-Q|z|}}{(Qv_{\perp})^2 + (\vec{Q}\cdot\vec{v}_{\parallel} - \omega)^2} \frac{1 - \bar{\epsilon}(Q, \omega)}{1 + \bar{\epsilon}(Q, \omega)}, \quad (1)$$

where  $\vec{v}_{\perp}$  and  $\vec{v}_{\parallel}$  are components of the velocity normal and parallel to the surface, respectively, and the position of the particle at time  $t$  is  $(v_{\parallel}t, 0, v_{\perp}t)$ . This expression is valid while the charge is outside the solid. It is evaluated by a standard electrodynamic self-energy argument in which the scalar potential generated in the medium by the particle is evaluated at the position of the particle and multiplied by one-half of its charge. We use atomic units throughout ( $e = \hbar = m = 1$ ).

Note also that the equivalent real part of the self-energy is denoted by  $\Sigma_r(\vec{r})$  in quantal treatments.<sup>17</sup> A quantity which has been termed the surface dielectric constant by News<sup>24</sup> is defined by

$$\bar{\epsilon}(Q, \omega) = \frac{Q}{\pi} \int_{-\infty}^{\infty} \frac{dk_{\perp}}{(k_{\perp}^2 + Q^2)\epsilon(k, \omega)}, \quad (2)$$

where  $k = (k_{\perp}^2 + Q^2)^{1/2}$ . Equation (1) gives the interaction energy of a charged particle with a surface in terms of the bulk dielectric constant  $\epsilon(\vec{k}, \omega)$ . Moreover, as found by Ritchie and Marusak,<sup>21</sup> the surface-plasmon dispersion relation is given by the solution of

$$\bar{\epsilon}(Q, \omega) + 1 = 0. \quad (3)$$

We could take any of the well-known dielectric functions for the bulk and solve Eq. (1) with  $\bar{\epsilon}(\vec{Q}, \omega)$  given by Eq. (2) (see the Appendix). In-

## DIELECTRIC FORMULATION

The model we take is that of a solid in the region  $z > 0$  characterized by a bulk dielectric function  $\epsilon(\vec{k}, \omega)$  and with vacuum in the region  $z < 0$ . We assume the surface of our model system to be located half of the interatomic distance outside of the last atomic layer of a real solid.

The classical self-energy  $\Phi_I(\vec{r})$  (the image potential) experienced by a charge  $Z_1 e$  moving in a fixed trajectory  $\vec{r} = \vec{v}t$  may be found from the specular reflection model. This model was first used to study the dispersive properties of the surface plasmon some time ago by Ritchie and Marusak<sup>21</sup> and was discussed independently by Wagner.<sup>22</sup> It has been shown to describe some properties of the electron gas with surprisingly good accuracy.<sup>23</sup> Many other workers have used this model subsequently to study various aspects of the image potential at a charge near a metal surface.<sup>10-12, 24, 25</sup> In this model, for a charge approaching the solid from vacuum,

instead, and in the spirit of the plasmon-pole approximation to the bulk dielectric constant,<sup>26</sup> we introduce a kind of surface-plasmon-pole approximation for  $\bar{\epsilon}(Q, \omega)$  given by

$$\bar{\epsilon}(Q, \omega) = 1 + \omega_p^2 / [\omega(\omega + i\gamma) - \omega_p^2 - \alpha Q - \beta Q^2 - Q^4/4], \quad (4)$$

where  $\omega_p$  is the bulk plasma frequency,  $\gamma$  is an infinitesimal damping constant, and  $\alpha$  is given by

$$\alpha = \sqrt{3/5} v_F \omega_s, \quad (5)$$

where  $v_F$  is the Fermi velocity and  $\omega_s = \omega_p / \sqrt{2}$  is the surface-plasmon frequency. This dielectric function reproduces the results of Ritchie and Marusak<sup>21</sup> and Inkson<sup>17</sup> for the surface-plasmon dispersion relation for small  $Q$  and takes into account single-particle response through the presence of the  $Q^4$  term.

Using Eq. (4) in Eq. (3) and solving for the resonant frequency  $\omega_s(Q)$ , one finds

$$\omega_s(Q) = (\omega_s^2 + \alpha Q + \beta Q^2 + Q^4/4)^{1/2}. \quad (6)$$

The  $Q^2$  term is added in Eq. (4) to force the surface-plasmon dispersion relation to join the single-particle continuum at the same point as the bulk line does, as prescribed by Wikborg and Inglesfield.<sup>27</sup> The values of the parameter  $\beta$  are given in Table I. A similar model without the  $Q^2$  term has been used by Barberan *et al.*,<sup>28</sup> to

TABLE I. Cutoff wave number versus  $r_s$ .  $Q_c$  is the value of the cutoff wave number at which the bulk plasmon dispersion curve enters the single-particle continuum. It is defined by  $\omega_p(Q_c) = Q_c(Q_c + 2k_F)/2$ , where  $\omega_p(k)$  is the volume plasmon frequency at wave vector  $k$ . The quantity  $\beta_{\text{exact}} = v_F^2 - (\alpha Q_c + \omega_s^2 - Q_c^2 v_F)/Q_c^2$  is chosen so that the analytical expression given in Eq. (6) passes through the point  $(\omega_p(Q_c), Q_c)$  in the  $(\omega-Q)$  plane. The analytical approximation  $\beta(r_s) = a + b/r_s^c$  is chosen so that agreement with  $\beta_{\text{exact}}(r_s)$  is obtained to two significant figures over the range of  $r_s$  shown. The constants were found to be  $a = 0.0026$ ,  $b = 2.6798$ , and  $c = 1.85$ . An analytical fit to  $Q_c(r_s)$  that gives comparable accuracy is  $Q_c = 0.9259/r_s^{1/2} + 0.2117/r_s - 0.0621$ .

$r_s$	$Q_c$	$\beta_{\text{exact}}$	$\beta = a + b/r_s^c$
2	0.6985	0.7458	0.7460
3	0.5424	0.3524	0.3537
4	0.4538	0.2090	0.2088
5	0.3937	0.1384	0.1391
6	0.3512	0.0999	0.100

study the influence of the image force on the trajectory of an electron in grazing-incidence reflection inelastic electron spectroscopy. Note that Eq. (6) appears to yield values of  $\omega_s(Q)$  that are somewhat too large compared with experiment<sup>15</sup> for  $Q \lesssim \omega_s^2/\alpha$ . The reason is presumably that the density profile of a real metal surface deviates from the step function variation assumed in Refs. 17 and 21. It would be a simple matter to fit observed dispersion curves using a form similar to Eq. (6). The surface dielectric function defined by Eq. (4) satisfies the sum rule  $\int_0^\infty \omega \text{Im}(-\tilde{\epsilon}) d\omega = \pi \omega_p^2/2$  as it must from the sum rule  $\int_0^\infty \omega \text{Im}(-1/\epsilon) d\omega = \pi \omega_p^2/2$  applied to Eq. (2).

Before analyzing the case of a moving charge, it is instructive to consider a fixed charge located at a distance  $z$  from the surface in vacuum. For this case the image potential becomes

$$\Phi_I(z) = -\frac{Z_1^2 \omega_s^2}{2} \int_0^\infty \frac{e^{-2Q|z|} dQ}{\omega_s^2 + \alpha Q + \beta Q^2 + Q^4/4}, \quad (7)$$

where we tentatively extend the integration to infinity. The contribution from the interval  $Q_c \leq Q < \infty$  amounts to  $\lesssim 30\%$  of that from the interval  $0 \leq Q \leq Q_c$  at metallic densities. Clearly as  $z \rightarrow -\infty$ ,

$$\Phi_I(z) \rightarrow -\frac{Z_1^2}{4|z|}, \quad (8)$$

which is the classical Coulombic image potential. For small values of  $z$ , the image potential differs significantly from its classical limit. The deviation from this result increases as  $|z|$  decreases. In Fig. 1 we have plotted  $\Phi_I(z)$  from Eq. (7) and the asymptotic form, Eq. (8), for the case of alumi-

num metal to illustrate how surface-plasmon dispersion and single-particle excitations affect the image potential with respect to its classical limit.

As stated above, although we plot  $\Phi_I(z)$  for both positive and negative values of  $z$ , it does not represent the true potential inside the solid ( $z > 0$ ). The potential there may be analyzed in terms of the contribution from virtual excitation of bulk plasmons as well as surface plasmons.<sup>15,20</sup> Recently, Eguluz<sup>29</sup> has studied the image potential for a static point charge at points outside and within the solid in the hydrodynamic approximation.

The potential at the origin can be approximated analytically as

$$\Phi_I(0) \approx -\frac{0.38Z_1^2}{r_s^{0.622}}. \quad (9)$$

This gives  $-6.57$  eV for the case of a proton interacting with a solid at the electron density of aluminum.

## HAMILTONIAN FORMULATION

### Real part

The total Hamiltonian of a system composed of a fast charged particle interacting with the surface may be approximated as<sup>30,31</sup>

$$H = H_p + H_{os} + H_{ps}, \quad (10)$$

where

$$H_p = p^2/2, \quad (11)$$

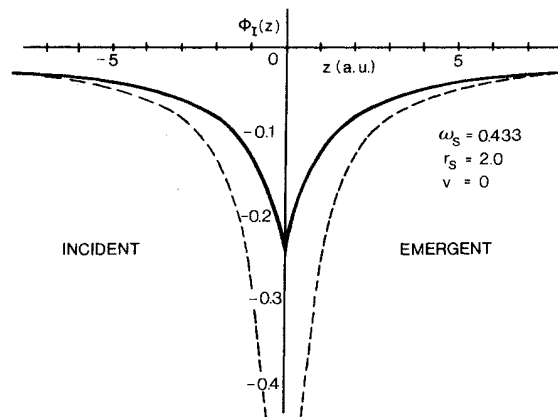


FIG. 1. Static image potential  $\Phi_I(z)$  vs  $z$  for a unit charge ( $Z_1 = 1$ ) at distance  $z$  from a metal surface. The solid line shows the results of calculations using Eq. (7). The dashed line is computed from the asymptotic expression, Eq. (8). For this case  $r_s = (3/4\pi n_0)^{1/3}$ , the one-electron radius in the equivalent electron gas, was taken to be 2.07. The electron density is  $n_0$ .

$$H_{0s} = \sum_{\vec{Q}} \omega_Q (a_{\vec{Q}}^\dagger a_{\vec{Q}} + \frac{1}{2}), \quad (12)$$

and

$$H_{ps} = \sum_{\vec{Q}} \Gamma(a_{\vec{Q}} e^{i(\vec{Q} \cdot \vec{b})} + \text{H.c.}). \quad (13)$$

Here

$$\Gamma_Q = C_Q e^{-Qv|t|}, \quad (14)$$

$\vec{p}$  is the incident particle momentum,

$$|\psi(t)\rangle = \prod_{\vec{Q}} \exp\left(-\int_{-\infty}^t ds I_{\vec{Q}}(s) \frac{dI_{\vec{Q}}^*(s)}{ds}\right) \exp[iI_{\vec{Q}}(t) a_{\vec{Q}}^\dagger] \exp(-iI_{\vec{Q}}^*(t) a_{\vec{Q}}) |\bar{\psi}(-\infty)\rangle, \quad (16)$$

where  $|\bar{\psi}(-\infty)\rangle$  represents the vacuum state of the surface-plasmon field when the incoming particle is at  $z = -\infty$ . The integral  $I_Q(t)$  is given by

$$I_{\vec{Q}}(t) = -i \int_{-\infty}^t \Gamma_Q(t_1) \exp[-i\vec{Q} \cdot \vec{b}(t_1) + i\omega_Q t_1] dt_1. \quad (17)$$

We define the real part of the image potential (i.e., the real part of the self-energy of the particle) as half of the expectation value of the scalar electric potential operator evaluated at the particle position, i.e.,

$$\begin{aligned} \Phi_I(\vec{r}(t)) &= \frac{1}{2} \langle \psi(t) | H_{ps} | \psi(t) \rangle \\ &= \sum_{\vec{Q}} \text{Re}[\Gamma_Q(t) I_{\vec{Q}}(t) e^{-i\omega_Q t}]. \end{aligned} \quad (8)$$

The same result for  $t < 0$  ( $z < 0$ ) could be obtained defining the image potential  $\Phi_I$  as<sup>20</sup>

$$\Phi_I = \langle \psi(t) | (H_{0s} + H_{ps}) | \psi(t) \rangle. \quad (19)$$

This definition gives the same result for  $z < 0$ , because in this case

$$\langle \psi(t) | H_{0s} | \psi(t) \rangle = -\Phi_I(\vec{r}(t)). \quad (20)$$

However, definition (19) cannot reproduce the results of a dielectric calculation once the particle has crossed the surface.<sup>19</sup> The value  $\langle \psi | H_{0s} | \psi \rangle$  is connected with the average number of real surface modes created and is related to the energy loss of the incident particle (i.e., to the imaginary part of the interaction energy).

The fact that Eq. (20) holds for negative times ( $z < 0$ ) is due to the particular form of the coupling constant  $\Gamma_Q(t)$ , and is not a general feature of particle-surface interactions.<sup>33,34</sup> We take Eq. (18) as the definition of the image potential for all times. The results obtained agree with those derived from electromagnetic theory. The factor  $\frac{1}{2}$  relates the scalar potential to the interaction energy, the so-called real part of the self-energy, in many-body language.

To keep the algebra simple, we treat the case of

$$C_Q = \left( \frac{Z_1^2 \pi \omega_s^2}{A Q \omega_Q} \right)^{1/2}, \quad (15)$$

while  $a_{\vec{Q}}^\dagger$  and  $a_{\vec{Q}}$  are creation and annihilation operators of a surface mode corresponding to wave vector  $\vec{Q}$ , and  $A$  is a normalization area. The swift particle is taken to have charge  $Z_1$  and to be located at  $\vec{r}(t) = (\vec{b}(t), z(t))$ .

The wave function of the surface modes can be solved exactly<sup>30,32</sup> in the interaction picture and is given by

normal incidence ( $z = vt$ ) and find

$$\begin{aligned} \Phi_I(z) &= -\frac{Z_1^2 \omega_s^2}{2} \int_0^\infty \frac{e^{-Q|z|} dQ}{\omega_Q (\omega_Q^2 + v^2 Q^2)} \\ &\quad \times \left[ \omega_Q e^{-Q|z|} + 2Qv \sin\left(\frac{\omega_Q z}{v}\right) \Theta(z) \right], \end{aligned} \quad (21)$$

where  $\Theta(z)$  is the Heaviside step function. For  $z < 0$  and  $|z| \gg v/\omega_s$  this equation reproduces the undispersed [ $\omega_s(Q) = \omega_s$ ] result for the dynamical image potential since at such distances the particle only couples effectively to the long-wavelength surface modes.<sup>7-9,11</sup> In this limit Eq. (21) reduces to

$$\Phi_I(z) = -\frac{Z_1^2 \omega_s}{2v} \left[ f(2\omega_s |z|/v) - 2 \sin\left(\frac{\omega_s z}{v}\right) g\left(\frac{\omega_s z}{v}\right) \Theta(z) \right], \quad (22)$$

where

$$f(x) = \int_0^\infty \frac{e^{-ux}}{1+u^2} du, \quad g(x) = \int_0^\infty \frac{u e^{-ux}}{1+u^2} du. \quad (23)$$

In Fig. 2 we show the results of a numerical calculation of  $\Phi_I(z)$  from Eq. (21) and compare with the  $\Phi_I(z)$  from Eq. (22). The difference in the results increases as the distance from the surface decreases. Once the particle has crossed the surface and penetrates into the metal (or penetrates into the vacuum for the case of a particle coming from inside the solid), the potential acquires an oscillatory component in agreement with the dielectric results of Mahan<sup>18</sup> but now, due to the inclusion of dispersion and single-particle effects in the medium response, does not show the unphysical divergence at the surface [see Eqs. (36) and (37) below]. Inclusion of single-particle effects produces a realistic potential for points near the surface even after the particle has crossed the surface. The wavelength of such oscillations will be of the order of

$$\lambda = 2\pi v/\omega_s. \quad (24)$$

Such oscillations, present in Mahan's dielectric

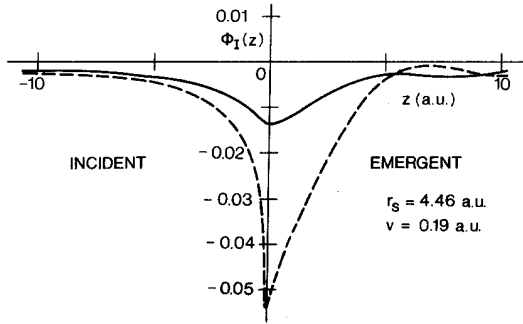


FIG. 2. Variation in  $\Phi_I(z)$ , the dynamic image potential appropriate to a particle of unit charge, plotted as a function of  $z$ . The dashed line corresponds to the neglect of dispersion, while the solid line shows results including dispersion and single particle excitations. The velocity  $v = 0.19$  a.u. is taken in the direction of positive  $z$  and  $\omega_s = 0.13$  a.u.

treatment of this problem, are smoothed out in the presence of dispersion.

#### Imaginary part

The imaginary part of the image potential accounts for the energy loss of the incident particle due to the creation of real surface excitations. The probability that a surface mode of momentum  $Q$  will have been excited at time  $t$  is given by [see Eq. (16)]

$$P_Q(t) = |I_Q(t)|^2. \quad (25)$$

The rate of transition to the final state  $a_Q^\dagger|0\rangle$  will be given by

$$\gamma_Q(t) = \frac{d}{dt} P_Q(t). \quad (26)$$

The energy absorbed at momentum  $Q$  per unit path length of the incident electron is then

$$\frac{dW}{dx} = \frac{\omega_Q}{v} \frac{dP_Q}{dt} \Big|_{\vec{r}=\vec{r}_t}. \quad (27)$$

We can simulate this energy loss of the incident particle by defining an absorptive part  $i\Sigma_i(z)$  of the image potential, where

$$\Sigma_i(z) \equiv \frac{v}{2} \sum_Q \frac{1}{\omega_Q} \frac{dW}{dx} = \frac{1}{2} \sum_Q \gamma_Q(t). \quad (28)$$

For the case of normal incidence, we have

$$\Sigma_i(z) \Big|_{z < 0} = -\frac{Z_1^2}{2} \omega_s^2 v \int_0^\infty \frac{Q e^{-2Q|z|} dQ}{\omega_Q (\omega_Q^2 + Q^2 v^2)}, \quad (29)$$

$$\Sigma_i(z) \Big|_{z > 0} = -\frac{Z_1^2}{2} \omega_s^2 v \int_0^\infty \frac{Q dQ}{\omega_Q (\omega_Q^2 + Q^2 v^2)} \times \left[ 2 \cos\left(\frac{\omega_Q z}{v}\right) e^{-Qz} - e^{-2Qz} \right]. \quad (30)$$

For  $|z| \gg v/\omega_s$ , we get the following formulas corresponding to the undispersed model  $\omega_s(Q) = \omega_s$ :

$$\Sigma_i(z) \Big|_{z < 0} = -\frac{Z_1^2}{2} \frac{\omega_s}{v} g\left(\frac{2\omega_s|z|}{v}\right), \quad (31)$$

$$\Sigma_i(z) \Big|_{z > 0} = \frac{Z_1^2}{2} \frac{\omega_s}{v} \left[ g\left(\frac{2\omega_s|z|}{v}\right) - 2g\left(\frac{\omega_s|z|}{v}\right) \cos\left(\frac{\omega_s z}{v}\right) \right]. \quad (32)$$

It is interesting to note here that Eq. (31) and the first term of Eq. (32) represent a "conservative" contribution to  $\Sigma_i$  in the following sense. Equation (31) arises because the incident particle gains energy in moving through a field that attracts it toward the surface for  $z < 0$ . That energy is extracted again as the particle moves away from the surface in the region  $z > 0$ . Hence Eq. (31) and the first term of Eq. (32) give a net zero result over the entire trajectory of the particle, leaving only the second term of Eq. (32) that represents the effect of real excitation of plasmons. For large  $z$  ( $z < 0$ ,  $|z| \gg v/\omega_s$ ), expression (31) reproduces the asymptotic form of Inkson's<sup>17</sup> quantum-mechanical result for normal incidence, i.e.,

$$\Sigma_i(z) = -vZ_1^2/8\omega_s z^2. \quad (33)$$

The average number of surface modes created is given by

$$\langle \eta(z) \rangle = -\frac{2}{v} \int_{-\infty}^z \Sigma_i(z') dz'. \quad (34)$$

This expression reproduces, in the undispersed model, Ritchie's original result<sup>35</sup>

$$\langle \eta(\infty) \rangle = \frac{\pi}{2v} Z_1^2. \quad (35)$$

Figure 3 shows the average number of modes for the case of a small velocity charge  $v = 0.19$  a.u. approaching a surface characterized by a surface plasma energy of 0.13 a.u. The average number of modes is much smaller than the result found neglecting dispersion. As the velocity of the incident particle increases, the undispersed model becomes nearer to our results. For the case of parallel incidence, of crucial importance in the case of RHEED experiments,<sup>30</sup> we get

$$\Sigma_{i||}(z) = -\frac{1}{2} \omega_s^2 Z_1^2 \int_0^\infty \frac{e^{-2Q|z|} \Theta(vQ - \omega_Q)}{\omega_Q (Q^2 v^2 - \omega_Q^2)^{1/2}} dQ. \quad (36)$$

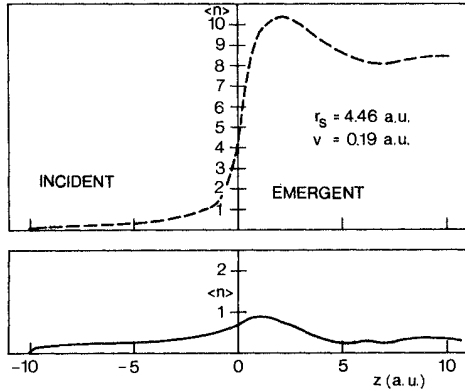


FIG. 3. Average number of surface modes  $\langle n(z) \rangle$ , created by a particle of unit charge having velocity  $v = 0.19$  a.u. ( $\omega_s = 0.13$  a.u.) as a function of distance from the surface. The velocity is taken in the direction of positive  $z$ . The dashed curve shows results neglecting dispersion and the solid curve corresponds to the inclusion of dispersion.

For large  $|z|$  this expression reproduces the result of Echenique and Pendry<sup>14</sup>

$$\Sigma_{i||}(z) = -\frac{Z_1^2 \omega_s}{2v} K_0\left(\frac{2\omega_s |z|}{v}\right), \quad (37)$$

where  $K_0$  is the Bessel function. This, in turn, has the same asymptotic limit as Inkson's expression for the imaginary part of the self-energy.<sup>17</sup>

Figure 4 shows the results of a calculation of the imaginary part of the self energy for a particle with  $v = 7$  a.u. moving perpendicular to a solid

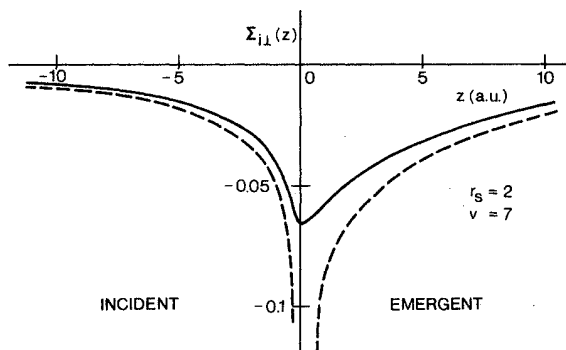


FIG. 4. Variation in  $\Sigma_{i\perp}(z)$ , the imaginary part of the self-energy of particle, as it depends on distance from the surface. The particle is taken to have unit charge and is normally incident on an aluminum surface. The velocity,  $v = 7$  a.u., is taken in the direction of positive  $z$ , and  $r_s = 2.07$ . The dashed curve shows results neglecting dispersion and the solid curve corresponds to the inclusion of dispersion.

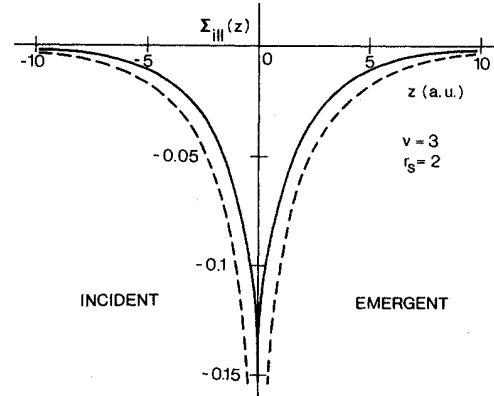


FIG. 5. Imaginary part of the surface potential,  $\Sigma_{i||}(z)$ , for a particle with unit charge traveling parallel to an aluminum surface. The velocity  $v = 3$ . The potential is plotted as a function of distance from the surface in vacuum. The dashed curve shows results neglecting dispersion and the solid curve corresponds to the inclusion of dispersion.

surface. In Fig. 5 we show the effect of including plasmon dispersion and single-particle effects on the imaginary part of the self-energy of a particle with velocity  $v = 3$  a.u. incident glancingly upon an aluminum surface.

## CONCLUSIONS

We have shown how plasmon dispersion and single-particle effects can be included in a simplified way in the study of the interaction of charged particles with solid surfaces. The introduction of the surface-plasmon-pole approximation allows us to obtain reasonably simple expressions with correct asymptotic behavior for both the real and imaginary parts of the surface potential. A good knowledge of such potential is important for a large variety of problems such as LEED and RHEED reflectivities and especially to the understanding of surface resonances.

Our analysis shows that dispersion and single-particle effects can reduce significantly the possibility of inelastic scattering, reducing the average number of surface modes created. The model presented here should also find very useful applications in the study of localized positron states at metal surfaces.<sup>36,37</sup>

## ACKNOWLEDGMENTS

The first two authors express their appreciation of the hospitality at the Cavendish Laboratory during the time some of this work was done. One of us (P.M.E.) wants to thank Professor J. J. Hopfield for a long, clarifying discussion about the defini-

tion of the real and imaginary parts of the surface potential. Thanks are also due to Professor Pedro Pascual and to J. C. Ashley for many helpful discussions. Research was sponsored in part by the Office of Health and Environmental Research, U.S. Department of Energy, under Contract No. W-7405-eng-26 with the Union Carbide Corporation.

#### APPENDIX

The surface dielectric constant is obtained from

$$\bar{\epsilon}(Q, \omega) = \frac{Q}{\pi} \int_{-\infty}^{\infty} \frac{(\omega^2 - \tilde{\beta}^2 k^2 - k^4/4) dk_{\perp}}{(Q^2 + k_{\perp}^2)(\omega^2 - \omega_p^2 - \tilde{\beta}^2 k^2 - k^4/4)}, \quad (\text{A1})$$

where we use the standard expression  $\epsilon(\omega, k) = 1 + \omega_p^2/(\tilde{\beta}^2 k^2 + k^4/4 - \omega^2)$  in the bulk plasmon-pole approximation.<sup>26</sup> The integral may be evaluated in a straightforward manner by deforming the  $k_{\perp}$  contour into the upper half-plane and evaluating the residues at the three simple poles enclosed. We find, when  $\tilde{\beta}^4 + \Omega^2 > 0$  and  $\tilde{\beta}^2 + Q^2/2 > (\tilde{\beta}^4 + \Omega^2)^{1/2}$

$$\bar{\epsilon} = \frac{\omega^2}{\Omega^2 + \Lambda_- - \Lambda_+} \left( \frac{1}{\Lambda_+(Q^2 - 2\Lambda_+)^{1/2}} - \frac{1}{\Lambda_-(Q^2 - 2\Lambda_-)^{1/2}} \right), \quad (\text{A2})$$

where

$$\Omega^2 = \omega^2 - \omega_p^2, \\ \Lambda_{\pm} = [\tilde{\beta}^2 \pm (\tilde{\beta}^4 + \Omega^2)^{1/2}].$$

When  $\tilde{\beta}^4 + \Omega^2 < 0$ ,

$$\bar{\epsilon} = \frac{\omega^2}{\Omega^2} - \frac{2Q\omega_p^2(Q^2 + c^2 - 3d^2)}{d(d^2 + c^2)[(Q^2 + c^2 - d^2)^2 + 4c^2d^2]}, \quad (\text{A3})$$

where

$$c = \frac{1}{\sqrt{2}}[(a^2 + b^2)^{1/2} + a]^{1/2}, \quad d = \frac{1}{\sqrt{2}}[(a^2 + b^2)^{1/2} - a]^{1/2},$$

and

$$a = -(Q^2 + 2\tilde{\beta}^2), \quad b = 2(|\tilde{\beta}^4 + Q^2|)^{1/2}.$$

For the case  $\tilde{\beta}^4 + \Omega^2 < 0$ , we find that  $\bar{\epsilon}$  is complex. We do not inquire into this case since here we are only interested in the real solution of the equation  $\bar{\epsilon} + 1 = 0$ . Thus we seek the solution  $\omega_Q$  of the equation  $\bar{\epsilon}(\omega_Q, Q) + 1 = 0$  only from  $\bar{\epsilon}$  as given in Eq. (A2). Although the resulting surface-plasmon-pole dispersion relation does not agree precisely with that found by substituting Eq. (4) in Eq. (3), it is linear in  $Q$  when  $Q$  is small and is represented reasonably well in general trend by Eq. (6). For convenience and in the spirit of the plasmon-pole approximation, we choose Eq. (6) to represent the surface dielectric function in this paper.

\*Present address: Facultad de Física, Universidad de Barcelona, Spain.

<sup>1</sup>A. A. Lucas, Phys. Rev. B **4**, 2939 (1971).

<sup>2</sup>G. D. Mahan, Phys. Rev. B **5**, 739 (1972).

<sup>3</sup>R. H. Ritchie, Phys. Lett. **A38**, 189 (1972).

<sup>4</sup>P. J. Feibelman, Surf. Sci. **27**, 438 (1971).

<sup>5</sup>N. G. Van Kampen, B. R. A. Nijboer, and K. Schram, Phys. Lett. **26A**, 307 (1968).

<sup>6</sup>E. Gerlach, Phys. Rev. B **4**, 393 (1971).

<sup>7</sup>R. Ray and G. D. Mahan, Phys. Lett. **A42**, 301 (1972).

<sup>8</sup>M. Sunjic, G. Toulouse, and A. A. Lucas, Solid State Commun. **11**, 1629 (1972).

<sup>9</sup>D. Chan and P. Richmond, Surf. Sci. **39**, 437 (1973).

<sup>10</sup>J. Harris and R. O. Jones, J. Phys. C **6**, 3585 (1973).

<sup>11</sup>J. Heinrichs, Phys. Rev. B **8**, 1346 (1973).

<sup>12</sup>D. Chan and P. Richmond, J. Phys. C **9**, 163 (1976).

<sup>13</sup>J. Rundgren and G. Malmström, Phys. Rev. Lett. **38**, 836 (1977).

<sup>14</sup>P. M. Echenique and J. B. Pendry, J. Phys. C **8**, 2936 (1975); P. M. Echenique, 1976, Ph. D. thesis, Cavendish Laboratory, Cambridge, United Kingdom (unpublished).

<sup>15</sup>P. J. Feibelman, C. B. Duke, and A. Bagchi, Phys. Rev. B **5**, 2436 (1972).

<sup>16</sup>J. C. Inkson, Surf. Sci. **28**, 69 (1971).

<sup>17</sup>J. C. Inkson, J. Phys. F **3**, 2143 (1973).

<sup>18</sup>C. H. Hodges, J. Phys. C **8**, 1849 (1975).

<sup>19</sup>F. Flores and F. García-Moliner, J. Phys. C **12**, 907 (1979).

<sup>20</sup>G. D. Mahan, *Collective Properties of Physical Systems* (Nobel Symposium No. 24) (Academic Press, New York, 1973), p. 164.

<sup>21</sup>R. H. Ritchie and A. L. Marusak, Surf. Sci. **4**, 234 (1966).

<sup>22</sup>D. Wagner, Z. Naturforsch. **21a**, 634 (1966).

<sup>23</sup>V. Celli, in *Surface Physics* (IAEA, Vienna, 1974), p. 393.

<sup>24</sup>D. M. News, Phys. Rev. B **1**, 3304 (1970).

<sup>25</sup>J. I. Gersten and N. Tzoar, Phys. Rev. B **8**, 5671 (1973).

<sup>26</sup>L. Hedin and S. Lunqvist, Solid State Phys. **23**, 1 (1969).

<sup>27</sup>E. Wikborg and J. E. Inglesfield, Phys. Scr. **15**, 37 (1977).

<sup>28</sup>N. Barberán, P. M. Echenique, and J. Viñas, J. Phys. C **12**, L 111 (1979).

<sup>29</sup>A. Eguluz, Solid State Commun. **33**, 21 (1980).

<sup>30</sup>A. A. Lucas, E. Kartheuser, and R. G. Badro, Phys. Rev. B **2**, 2488 (1970).

<sup>31</sup>M. Sunjic and A. A. Lucas, Phys. Rev. B **3**, 719 (1971).

<sup>32</sup>A. Galindo and P. Pascual, *Mecánica Cuántica* (Editorial Alhambra, Madrid, Spain, 1978).

<sup>33</sup>M. W. Cole, Phys. Rev. B 2, 4239 (1970).

<sup>34</sup>P. M. Echenique and J. B. Pendry, Phys. Rev. Lett. 37, 561 (1976); P. M. Echenique and J. B. Pendry, J. Phys. C 9, 3183 (1976).

<sup>35</sup>R. H. Ritchie, Phys. Rev. 106, 874 (1957).

<sup>36</sup>J. B. Pendry (unpublished).

<sup>37</sup>N. Barberán and P. M. Echenique, Phys. Rev. B 19, 5431 (1979).